

Electrochemical Studies of Hydrogen Chloride Gas in Several Room Temperature Ionic Liquids: Mechanism and Sensing

Krishnan Murugappan^{1,2}, Debbie S. Silvester^{1}*

¹ Nanochemistry Research Institute, Department of Chemistry, Curtin University, GPO Box
U1987, Perth, 6845, Australia.

² Present address: Department of Materials, Parks Rd, Oxford OX1 3PH, United Kingdom.

*Email: d.silvester-dean@curtin.edu.au, Phone: +61(8)92667148

Submitted to: Physical Chemistry Chemical Physics.

Electrochemical Studies of Hydrogen Chloride Gas in Several Room Temperature Ionic Liquids: Mechanism and Sensing

Abstract

The electrochemical behaviour of highly toxic hydrogen chloride (HCl) gas has been investigated in six room temperature ionic liquids (RTILs) containing imidazolium/pyrrolidinium cations and range of anions on a Pt microelectrode using cyclic voltammetry (CV). HCl gas exists in a dissociated form of H^+ and $[\text{HCl}_2]^-$ in RTILs. A peak corresponding to the oxidation of $[\text{HCl}_2]^-$ was observed, resulting in the formation of Cl_2 and H^+ . These species were reversibly reduced to H_2 and Cl^- , respectively, on the cathodic CV scan. The H^+ reduction peak is also present initially when scanned only in the cathodic direction. In the RTILs with a tetrafluoroborate or hexafluorophosphate anion, CVs indicated a reaction of the RTIL with the analyte/electrogenerated products, suggesting that these RTILs might not be suitable solvents for the detection of HCl gas. This was supported by NMR spectroscopy experiments, which showed that the hexafluorophosphate ionic liquid underwent structural changes after HCl gas electrochemical experiments. The analytical utility was then studied in 1-ethyl-3-methylimidazolium bis(trifluoromethylsulfonyl)imide ($[\text{C}_2\text{mim}][\text{NTf}_2]$) by utilising both peaks (oxidation of $[\text{HCl}_2]^-$ and reduction of protons) and linear calibration graphs for current vs concentration for the two processes were obtained. The reactive behaviour of some ionic liquids clearly shows that the choice of the ionic liquid is very important if employing RTILs as solvents for HCl gas detection.

Keywords: Hydrogen Chloride • Room Temperature Ionic Liquids • Cyclic Voltammetry • Reaction Mechanism • Electrochemistry • Gas Sensing

1. Introduction

Hydrogen chloride (HCl) is a colourless toxic gas with a strong pungent odour. The current USA Occupational Safety and Health Administration Permissible Exposure Limit (OSHA PEL) for HCl gas is 5 ppm. HCl is highly corrosive, and in the presence of moisture forms hydrochloric acid which causes burns and irritation to the skin and is corrosive to the eyes and mucous membranes.^{1, 2} Ulceration of the nose, throat and larynx can occur upon excess inhalation³ and frequent exposure can cause dermatitis.³ Concentrations above 15,000 ppm are deadly to humans and contact for more than 1 hour should be avoided at concentrations of 50 ppm and above.³ In addition to the harmful effects on humans, it also causes corrosion to metals (e.g. iron)³ and needs to be closely monitored in industry.

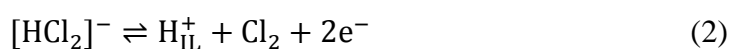
There are several ways to prepare hydrogen chloride gas such as reacting sulphuric acid with sodium chloride or by reacting chlorine with hydrogen at temperatures above 250°C.^{3, 4} HCl is used in the gasoline industry as a precursor for the formation of aluminium chloride catalyst which converts *n*-butane to isobutane.³ HCl is also used in the electronic industry as an etchant for semiconductor materials.³ In the textile industry, HCl gas is used to disinfect cotton seeds and also to decompose vegetable fibres in wool so that they can be reclaimed for use in fabrics.³ In the metal industry it is used to clean metals due to its strong disinfectant properties.³ As a result of its high toxicity and use in many industries, it is essential to be able to detect and monitor hydrogen chloride gas.

There have been very limited studies on the electrochemical behaviour of HCl gas in aprotic solvents. Michlmayr and Sawyer⁵ reported electrochemistry of HCl on Pt in anhydrous dimethylsulfoxide (DMSO) and acetonitrile, and observed one oxidation and one reduction peak. They assigned the behaviour to the dissociation of HCl to H⁺ and Cl⁻, followed by the reduction of H⁺ (at ca. -0.9 V vs SCE) and oxidation of Cl⁻ (at ca. +0.6 V vs. SCE). They

suggested that follow-up chemical reactions with the solvent occurred after the oxidation step. In room temperature ionic liquids (RTILs), the only report is on the electrochemical behaviour of a saturated solution of hydrogen chloride in 1-butyl-3-methylimidazolium bis(trifluoromethylsulfonyl)imide ([C₄mim][NTf₂]) on a Pt macrodisk electrode by Aldous et al.⁶ Four voltammetric peaks (two oxidation and two reduction) were observed in the first scan and five peaks (three oxidation and two reduction) were observed in the second scan. All processes were diffusion controlled. It is believed that HCl dissociates to form [HCl₂]⁻ and H⁺ when dissolved in the RTIL according to equation 1:⁶



The oxidation peak at ca. 1.9 V vs. (Ag/Ag⁺) was attributed to the two-electron oxidation of [HCl₂]⁻, forming protons solvated by the ionic liquid (H_{IL}⁺) and chlorine gas (equation 2):



When the scan was reversed two reduction peaks corresponding to the reduction of chlorine and protons, respectively, were observed. Both of these processes were chemically reversible, with Cl⁻ oxidation and H₂/H_{ads} peaks observed on the oxidation scan. It was reported that in these experiments there was difficulty in controlling the concentration of HCl in the RTIL. This could have been due to the nature of the experiments where HCl was bubbled directly into the RTIL and the cell was not at a constant atmosphere of HCl. Therefore rapid desorption of HCl took place, which prevented further mechanistic or analytical studies to be performed.

In this work the electrochemical behaviour of hydrogen chloride gas will be investigated in several room temperature ionic liquids to expand the knowledge of the mechanism in different RTILs on a Pt microelectrode. The analytical utility will also be investigated for the

first time in RTILs, opening up possibilities for using RTILs in amperometric gas sensors to detect low concentrations of hydrogen chloride gas.

2. Experimental Section

2.1 Chemical Reagents

The RTILs 1-ethyl-3-methylimidazolium bis(trifluoromethylsulfonyl)imide ($[\text{C}_2\text{mim}][\text{NTf}_2]$), 1-butyl-3-methylimidazolium bis(trifluoromethylsulfonyl)imide ($[\text{C}_4\text{mim}][\text{NTf}_2]$) and *N*-butyl-*N*-methylpyrrolidinium bis(trifluoromethylsulfonyl)imide ($[\text{C}_4\text{mpyrr}][\text{NTf}_2]$) were synthesized according to standard literature procedures^{7, 8} and kindly donated by the group of Professor Christopher Hardacre at Queens University, Belfast. The RTILs 1-hexyl-3-methylimidazolium trifluorotris(pentafluoroethyl)phosphate ($[\text{C}_6\text{mim}][\text{FAP}]$), 1-butyl-3-methylimidazolium hexafluorophosphate ($[\text{C}_4\text{mim}][\text{PF}_6]$) and 1-butyl-3-methylimidazolium tetrafluoroborate ($[\text{C}_4\text{mim}][\text{BF}_4]$) were purchased from Merck KGaA (Kilsyth, Victoria, Australia) at ultra-high purity electrochemical grade. Ultra-pure water with a resistance of 18.2 $\text{M}\Omega\cdot\text{cm}$ prepared by an ultra-pure laboratory water purification system (Millipore Pty Ltd., North Ryde, NSW, Australia) and acetonitrile (MeCN, Sigma–Aldrich, 99.8%) were used for washing the electrodes before and after use with RTILs. HCl gas (from two cylinders of concentrations 5 % and 0.2 %, the remainder being made of nitrogen) was purchased from CAC gases (Auburn, NSW, Australia). High purity nitrogen gas (99.9 %) was purchased from BOC gases (North Ryde, NSW, Australia). Ferrocene ($\text{Fe}(\text{C}_5\text{H}_5)_2$, 98 % purity) and tetra-*N*-butylammonium perchlorate (TBAP, 98 % purity) were from Sigma Aldrich.

2.2 Electrochemical Experiments

Electrochemical experiments were conducted using a PGSTAT101 Autolab (Eco Chemie, Netherlands) interfaced to a PC with NOVA 1.9 software. Experiments were conducted at a temperature of 295 (± 2) K inside an aluminium Faraday cage placed inside a fume cupboard.

A two-electrode arrangement was employed, with a home-made platinum microelectrode (8.3 μm radius) as the working electrode and a 0.5 mm diameter silver wire (Sigma Aldrich) as the quasi-reference electrode. The microelectrode was polished on soft lapping pads (Buehler, Illinois) with alumina powder of decreasing size (3, 1 and 0.5 μm , Kemet, NSW, Australia) before electrochemical experiments. The steady-state voltammetry of a 2 mM ferrocene (diffusion coefficient $2.3 \times 10^{-5} \text{ cm}^2\text{s}^{-1}$ at 298K)⁹ solution in acetonitrile with 0.1 M TBAP as the electrolyte was analysed to calibrate the electrode diameter. The electrodes were housed in a glass “T-cell” designed for studying microlitre quantities (30 μL used in this work) of ionic liquids in a controlled environment, previously used to study methylamine¹⁰ and chlorine¹¹ gas. Before gas was introduced, the cell was purged under high vacuum (Edwards high vacuum pump, model ES 50) to remove any impurities in the ionic liquid (e.g. dissolved water and oxygen from atmospheric moisture).

2.3 Gas Mixing Setup

A similar gas mixing setup as used previously for chlorine¹¹ was used for these experiments. The % concentration of hydrogen chloride that was introduced into the T-cell was calculated using the relative flow rates of the two flow meters. A digital flowmeter (0-1.2 L/min, John Morris Scientific, NSW, Australia) was used for the nitrogen gas and an analogue flowmeter (0-60 cm^3/min , Dwyer, NSW, Australia) was used for the hydrogen chloride gas. It took approximately 90 minutes for saturation to occur in most of the ionic liquids and the time taken between each concentration change was 45 minutes. This was to ensure that the RTIL

was fully saturated with gas. Hydrogen chloride is an extremely corrosive gas and reacts with moisture to form HCl and HClO, which corrodes steel to form rust. Therefore all Swagelok fittings that were connected to the hydrogen chloride gas flowmeter were made of PTFE. Experiments were also performed in the presence of a deep purge system (DPS) to flush the whole system with nitrogen gas before and after experiments so that no residual gases or moisture are present (as this can cause corrosion of all the metal fittings and regulator).

2.4 Nuclear Magnetic Resonance Experiments

Nuclear magnetic resonance (NMR) spectra were recorded using a Bruker Avance 400 spectrometer. 1 mL of deuterated chloroform (CDCl_3) was used to dissolve 5 μL of the RTIL ($[\text{C}_2\text{mim}][\text{NTf}_2]$, $[\text{C}_4\text{mim}][\text{BF}_4]$ and $[\text{C}_4\text{mim}][\text{PF}_6]$) in a NMR sample tube and experiments were conducted on the RTILs before and after electrochemical experiments with HCl. For the RTIL $[\text{C}_2\text{mim}][\text{NTf}_2]$, ^{13}C and ^1H spectra were obtained. For the RTIL $[\text{C}_4\text{mim}][\text{PF}_6]$, ^{13}C , ^1H , ^{31}P and ^{19}F spectra were obtained. For the RTIL, $[\text{C}_4\text{mim}][\text{BF}_4]$ ^{13}C , ^1H , ^{11}B and ^{19}F spectra were obtained. The relevant NMR spectra for $[\text{C}_4\text{mim}][\text{PF}_6]$ are shown in the supporting information (Figure S1).

3. Results and Discussion

The electrochemistry of hydrogen chloride gas has been investigated in six different RTILs, namely $[\text{C}_2\text{mim}][\text{NTf}_2]$, $[\text{C}_4\text{mim}][\text{NTf}_2]$, $[\text{C}_6\text{mim}][\text{FAP}]$, $[\text{C}_4\text{mpyrr}][\text{NTf}_2]$, $[\text{C}_4\text{mim}][\text{BF}_4]$, and $[\text{C}_4\text{mim}][\text{PF}_6]$ on a Pt microelectrode.

3.1 Electrochemical Behaviour of HCl Gas in Various RTILs

Figure 1 shows the cyclic voltammograms (CVs) of 2.56 % HCl gas (nitrogen fill) in six different RTILs ($[\text{C}_2\text{mim}][\text{NTf}_2]$, $[\text{C}_4\text{mim}][\text{NTf}_2]$, $[\text{C}_6\text{mim}][\text{FAP}]$, $[\text{C}_4\text{mpyrr}][\text{NTf}_2]$, $[\text{C}_4\text{mim}][\text{BF}_4]$, and $[\text{C}_4\text{mim}][\text{PF}_6]$) on a Pt microelectrode at a scan rate of 0.1 V/s when

scanned from 0 to 2.3 V (3 V in the case of [C₆mim][FAP]) to -1.8 V and back to 0 V. The thick solid line shows the first scan and the dashed line shows the second scan. The response in the absence of HCl is shown as the thin solid line. It can be seen that in all the RTILs on the first scan there is a broad oxidation peak (I) at approximately +2 V which is attributed to the two electron oxidation of [HCl₂]⁻ to form protons and chlorine gas (equation 2).⁶ The reasonably high currents obtained at concentrations of 2.56 % in the gas phase suggests a high solubility of hydrogen chloride which is very advantageous for sensing applications and will be explored later in section 3.4. The oxidation peak (I) is peak-shaped instead of sigmoidal, which is a common feature of voltammetry in RTILs,¹² where higher viscosities result in slower diffusion coefficients of electroactive species, meaning that true steady-state behaviour is not obtained. When the scan is reversed at 2.3 V there is a steady state reduction wave (III) at ca. -0.5 V corresponding to the reduction of protons. There is also a small peak (II) of approximately +0.9 V, corresponding to the reduction of electrogenerated chlorine. Both processes II and III have corresponding oxidation peaks (labelled IV and V).

It is important to note here that process II and process IV are not easily visible due to the much smaller electrode used in our experiments as compared to the work performed by Aldous et al.⁶ However these peaks do become obvious at higher scan rates, as will be discussed in the next section, and also on larger electrodes (e.g. on 4 mm diameter screen-printed electrodes).¹³

On the second scan (thick dashed line in figure 1) there is an additional peak (V) at ca. 1.2 V that is not present on the first scan. The appearance of this peak causes peak I to have a slightly higher peak current on the second scan compared to the first scan. Peak V is attributed to the oxidation of the chloride ions that are formed from peak II (reduction of chlorine). The absence of peak V on the first scan suggests that chloride is not present

initially in the RTIL, consistent with that suggested by Aldous et al.⁶ Table 1 summarises the reactions (previously proposed)⁶ for each peak.

Although the behaviour in all the RTILs is quite similar, there are some significant differences in some ionic liquids. For example peak I in [C₆mim][FAP] is not very evident compared to the other peaks. This could suggest a low solubility in this RTIL, however, peak III is clearly seen, so the more likely explanation is that peak I is very close to the edge of the available electrochemical window. In [C₄mim][BF₄], the potential separation between peaks I and V is the smallest of all the RTILs, and peak V is partly evident on the first scan (as a shoulder on peak I), suggesting that the mechanism may be slightly different in this RTIL. In the RTIL [C₄mim][PF₆] there are some major differences, with the main reduction features (between ca. -0.5 and -1 V) appearing to be very different compared to the other RTILs, which again suggests a different mechanism, probably caused by reactions with the RTIL itself. Since HCl gas dissociates into H⁺ and [HCl₂]⁻ in the RTIL, the environment is very acidic. It is known that [PF₆]⁻ and [BF₄]⁻ anions can dissociate to produce HF in acidic environments.^{14, 15} Furthermore, in [C₄mim][BF₄], and [C₄mim][PF₆], it was not possible to obtain featureless blanks (RTIL under vacuum) after HCl gas experiments were performed, as shown in Figure 2. This suggests that the RTILs have undergone a change, possibly explaining the difference in behaviour seen in those two RTILs for HCl oxidation. For comparison, the blank scans before and after HCl experiments were identical in the other four ionic liquids (CVs not shown). In figure 2, the first scan for the oxidation of 2.56 % HCl gas is also overlaid. It can be seen that blank [C₄mim][PF₆] (after HCl experiments) has peaks at -1 V and between 0 and -0.8 V, which have much higher currents than those observed in the presence of HCl gas. These large peaks could be due to the by-products of the ‘chemically transformed’ RTIL after HCl experiments.

In order to further characterise the RTILs before and after experiments, nuclear magnetic resonance (NMR) spectroscopy was performed in an attempt to observe structural changes in the RTILs. The NMR spectra of [C₄mim][PF₆] for ¹³C, ¹H, ³¹P and ¹⁹F were performed and the “before and after HCl” ¹H, ³¹P and ¹⁹F spectra can be found in the supporting information (figure S1). The NMR sample ‘before’ refers to the neat RTIL before any experiments with HCl, and the sample ‘after’ refers to the RTIL after electrochemical experiments with HCl, followed by nitrogen purging (to remove HCl from the system). From the ¹H spectrum (chemical shift between 9 and 11.5) it can be seen that there are no features in the RTIL before experiments. However after electrochemical experiments with HCl there is a feature at $\delta=11.5$ ppm that can be attributed to hydrogen bonding.¹⁶ Previous work was performed by Shenderovich et al.¹⁶ on HF and tetrabutylammonium fluoride, who attributed features between $\delta=10$ and $\delta=17$ to hydrogen bonding with the fluoride anion, most likely from the HF molecule. In order to form HF in our system, H⁺ ions must remove fluorine from [PF₆]⁻. This was further supported by the NMR spectrum of ³¹P and ¹⁹F (Figure S1b and S1c) where the ratio of the peaks before and after experiments were not the same, suggesting that PF₆ has become PF_{6-n} (where n is less than 5). This supports the suggestion that [C₄mim][PF₆] has undergone a structural change and is not a suitable solvent for HCl gas sensing. NMR for “before and after” HCl experiments in [C₄mim][NTf₂] and [C₄mim][BF₄] showed no obvious changes, suggesting that if HF forms in [C₄mim][BF₄], NMR was not sensitive enough to observe the changes.

3.2 Oxidation of HCl Gas in RTILs at Various Scan Rates

To further investigate the reaction mechanism of HCl gas, CV at a range of scan rates was performed in all the six RTILs for the first scan (supporting information, figure S2) and second scan (figure 3) at a range of scan rates from 0.05 V/s to 2 V/s. It can be seen clearly that as the scan rates increase, the currents for all processes increase. Peaks II and IV, which

were not very evident in figure 1 due to the lower scan rate used, become more evident at higher scan rates as shown in figure 3.

In [C₄mim][PF₆], the voltammetry at different scan rates is very different to the other RTILs, supporting the suggestion of structural changes to the RTIL in the presence of HCl. In the other five RTILs, it can be clearly seen that peak III (reduction of protons) splits into two processes at higher scan rates. The splitting of peaks was reported by Silvester et al.¹⁵ and Aldous et al.⁶ who attributed this to two competing reactions (equations 4/5 and 6, see table 1). All other features are the same in both the first and second scans at different scan rates.

Due to the peaks being well-defined in [C₂mim][NTf₂], [C₄mim][NTf₂] and [C₄mpyrr][NTf₂], further analysis was performed on these RTILs. The current obtained for peak I (first scan and second scan), peak V (second scan) and peak III (first scan) for the three RTILs ([C₂mim][NTf₂] (figure S3), [C₄mim][NTf₂] (figure S4) and [C₄mpyrr][NTf₂] (figure S5)) at the various scan rates was plotted against the square root of scan rate. In all figures the plots do not go through zero which is a common feature of voltammetry at microelectrodes in RTILs, where the behaviour is somewhere in-between pure microelectrode (steady state) and pure macroelectrode (transient).¹⁷ The plot of peak I (second scan) oxidation peak current vs square root of scan rate (figure S3b, S4b and S5b) has a higher R² value for the line of best fit as compared to the first scan (figure S3a, S4a and S5a) for all three ionic liquids. This is probably due to the addition of peak V just before peak I, which adds to the peak current, especially at high scan rates. This is most obvious in the RTIL [C₄mpyrr][NTf₂] (figure S2) where the plot of current vs. square root of scan rate (figure S5b) has the lowest R² value. Good linearity was observed (R² values ca. 0.99), suggesting that the electrochemical processes are most likely diffusion controlled, consistent with that reported by Aldous et al.⁶

3.4 Analytical Utility of HCl Gas in [C₂mim][NTf₂]

Once the fundamental electrochemical behaviour was understood, the analytical utility of hydrogen chloride was studied in [C₂mim][NTf₂] due to it being the least viscous RTIL available and one where all five processes are clearly defined. Voltammetry was recorded at a scan rate of 0.1 V/s. Figure 4 shows typical CVs for six different concentrations (104-1048 ppm) of HCl on a Pt microelectrode for both the first and second scan for each concentration. At this scan rate, the currents for both first and second scans are very similar and they almost overlap. However there is a slight increase in the current for peak I on the second scan due to the contribution of the chloride oxidation peak (V). As the concentration increases, the currents for all processes increase. A plot of peak current vs concentration (calibration graph) was obtained for both peak I (first scan) and peak III (first scan) and they are shown in the inset to figure 4. Linear behaviour is observed ($R^2 > 0.99$), with sensitivities of 1.99×10^{-12} and 1.75×10^{-12} A/ppm, for peak I and peak III, respectively. Due to the complicated oxidation mechanism, it was originally unclear if the calibration plots would be linear, however, excellent linearity was observed which is very important for sensing applications. Limits of detection (LODs) of 102 and 69 ppm were obtained for process I and process III, respectively. At the lower concentrations studied (104, 168ppm and 242 ppm) it was very hard to determine the peak current for peak I as the peak was not well defined. However there were no such issues with peaks III. This together with the LODs obtained suggests that measuring the currents from peak III (reduction of protons) might be a better alternative to using the [HCl₂]⁻ oxidation peak (I). We have recently demonstrated this by studying the behaviour of HCl gas at much lower concentrations (10-80 ppm) on a Pt screen-printed electrode,¹³ using the current for reduction of protons as the analytical response. LODs between ca. 1-3 ppm were achieved in [C₂mim][NTf₂], below the 5 ppm long-term exposure limit for HCl. This suggests that (some) RTILs may indeed be suitable solvents for HCl gas sensing, provided the anions and cations are stable in highly acidic environments.

4. Conclusions

The electrochemical behaviour of hydrogen chloride gas has been studied in six RTILs. In three RTILs ideal voltammetry was observed with a two electron oxidation of $[\text{HCl}_2]^-$ to Cl_2 and H^+ that are reversibly reduced on the reductive scan. Three of the RTILs were deemed not suitable for HCl gas sensing; $[\text{C}_6\text{mim}][\text{FAP}]$ due to the oxidation peak not being well defined, $[\text{C}_4\text{mim}][\text{BF}_4]$ and $[\text{C}_4\text{mim}][\text{PF}_6]$ because of possible reaction of HCl gas (or its reaction by-products) with the ionic liquid. NMR spectroscopy confirmed that $[\text{C}_4\text{mim}][\text{PF}_6]$ underwent structural changes after electrochemical experiments with HCl.

The analytical utility was also studied in $[\text{C}_2\text{mim}][\text{NTf}_2]$. Linear calibration graphs were obtained with LODs of 102 ppm and 69 ppm using the currents from the oxidation of $[\text{HCl}_2]^-$ and reduction of H^+ , respectively. The reduction of protons could be a more viable method to detect HCl gas due to more linear response and the oxidation of $[\text{HCl}_2]^-$ being at very high potentials. Overall, this work suggests that the choice of the RTIL is vital when exploring analytes with a highly acidic nature, such as HCl.

Acknowledgements

K.M. thanks Curtin University for the award of a Curtin International Postgraduate Research Scholarship and D.S.S. thanks the Australian Research Council for funding via a Discovery Early Career Research Award (DE120101456).

Footnotes

Electronic Supplementary Information: ^{19}F , ^1H and ^{31}P NMR spectra for experiments in $[\text{C}_4\text{mim}][\text{PF}_6]$ before and after electrochemical experiments with HCl. First scan CVs at different scan rates for the oxidation of HCl gas in six RTILs, and plots of peak current vs. square root of scan rate for peaks I, III and IV in three RTILs.

Tables

Table 1: Summary of peak labels and assignments.

Peak	Equation	Assigned reactions ⁶
I	2	$[\text{HCl}_2]^- \rightleftharpoons \text{H}_{\text{IL}}^+ + \text{Cl}_2 + 2\text{e}^-$
II	3	$\text{Cl}_{2\text{gas}} + 2\text{e}^- \rightleftharpoons 2\text{Cl}^-$
III	4	$\text{H}_{\text{IL}}^+ + \text{e}^- \rightleftharpoons \text{H}_{\text{ads}}$
	5	and $2\text{H}_{\text{ads}} \rightleftharpoons \text{H}_{2\text{gas}}$
	6	or $\text{H}_{\text{ads}} + \text{H}_{\text{IL}}^+ + \text{e}^- \rightleftharpoons \text{H}_{2\text{gas}}$
IV	7	Reverse of peak III
V	8	$2\text{Cl}^- \rightleftharpoons \text{Cl}_{2\text{gas}} + 2\text{e}^-$

List of Figures

Figure 1: CVs for the oxidation of 2.56 % hydrogen chloride gas (nitrogen fill) on a 8.3 μm radius Pt electrode in a) $[\text{C}_2\text{mim}][\text{NTf}_2]$, b) $[\text{C}_4\text{mim}][\text{NTf}_2]$, c) $[\text{C}_6\text{mim}][\text{FAP}]$, d) $[\text{C}_4\text{mpyr}][\text{NTf}_2]$, e) $[\text{C}_4\text{mim}][\text{BF}_4]$ and f) $[\text{C}_4\text{mim}][\text{PF}_6]$ at a scan rate 0.1 V/s. The thick solid line is the first scan, the thick dashed line is the second scan and the thin solid line is the blank (response in the absence of hydrogen chloride gas before experiments). The labels for peaks (I) to (V) are not included for $[\text{C}_4\text{mim}][\text{PF}_6]$ (f) due to different reactions occurring in this RTIL (see discussion).

Figure 2: CVs showing changes in blank scans (RTIL under vacuum conditions) for the oxidation of 2.56 % hydrogen chloride gas on a 8.3 μm radius Pt electrode in a) $[\text{C}_4\text{mim}][\text{BF}_4]$ and b) $[\text{C}_4\text{mim}][\text{PF}_6]$ at a scan rate 0.1 V/s. The thin black line is the blank scan before HCl gas and the thick dashed line is blank scan after HCl gas experiments.

Figure 3: CVs for the oxidation (second scan) of 2.56 % hydrogen chloride gas on a 8.3 μm radius Pt electrode in a) $[\text{C}_2\text{mim}][\text{NTf}_2]$, b) $[\text{C}_4\text{mim}][\text{NTf}_2]$, c) $[\text{C}_6\text{mim}][\text{FAP}]$, d) $[\text{C}_4\text{mpyr}][\text{NTf}_2]$, e) $[\text{C}_4\text{mim}][\text{BF}_4]$, f) $[\text{C}_4\text{mim}][\text{PF}_6]$ at various scan rates between 0.05 and 2 V/s. The labels for peaks (I) to (V) are not included for $[\text{C}_4\text{mim}][\text{PF}_6]$ (f) due to different reactions occurring in this RTIL.

Figure 4: CVs (first and second scan) for the oxidation of different concentrations (104, 168, 242, 431, 710 and 1048 ppm) of HCl gas on a 8.3 μm radius Pt electrode in $[\text{C}_2\text{mim}][\text{NTf}_2]$ at a scan rate 0.1 V/s. Insets are calibration graphs of current for peak I (first scan) and peak III (first scan) vs. gas phase concentration.

Figures

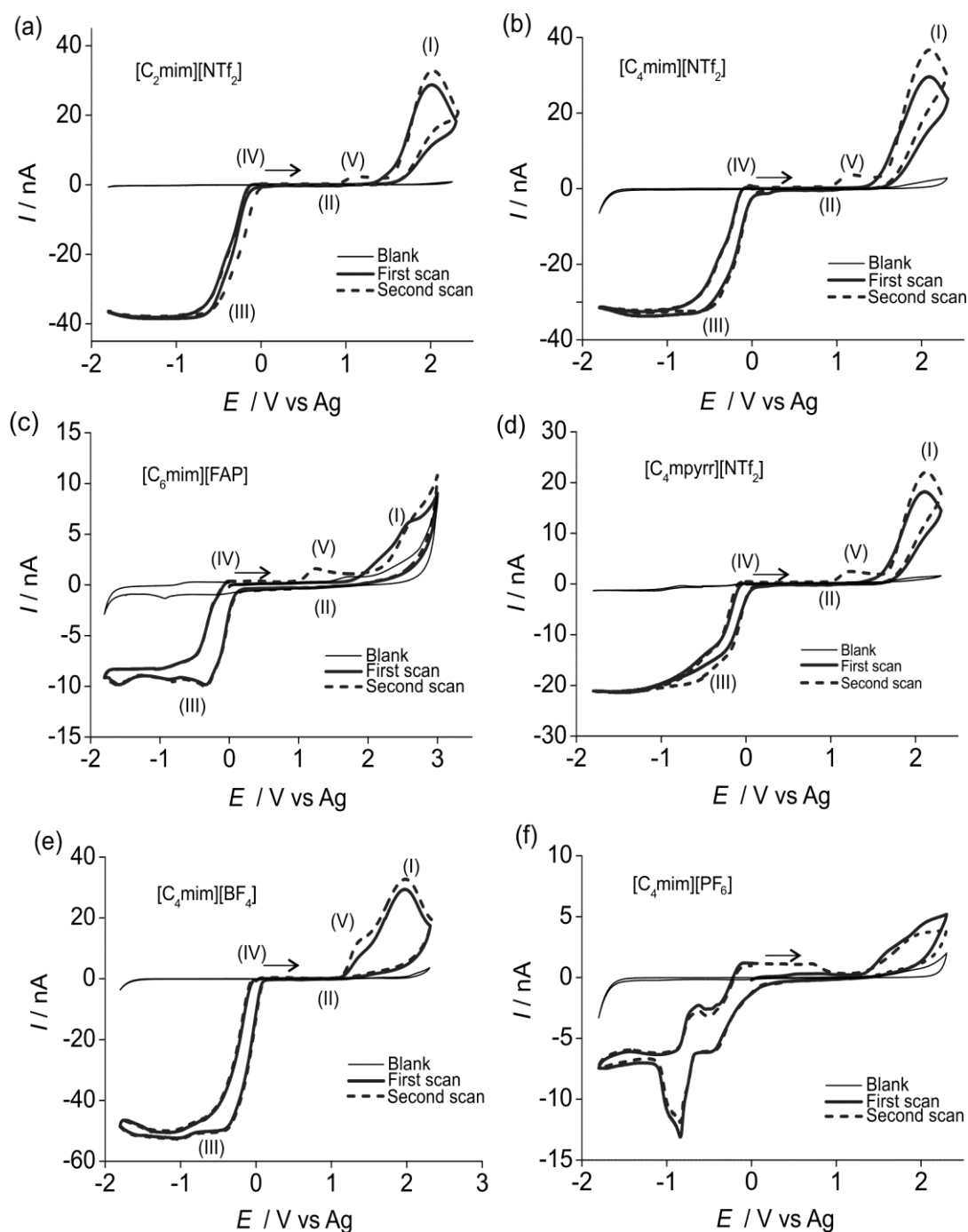


Figure 1: CVs for the oxidation of 2.56 % hydrogen chloride gas (nitrogen fill) on a 8.3 μ m radius Pt electrode in a) $[C_2mim][NTf_2]$, b) $[C_4mim][NTf_2]$, c) $[C_6mim][FAP]$, d) $[C_4mpyrr][NTf_2]$, e) $[C_4mim][BF_4]$ and f) $[C_4mim][PF_6]$ at a scan rate 0.1 V/s. The thick solid line is the first scan, the thick dashed line is the second scan and the thin solid line is the blank (response in the absence of hydrogen chloride gas before experiments). The labels for peaks (I) to (V) are not included for $[C_4mim][PF_6]$ (f) due to different reactions occurring in this RTIL (see discussion).

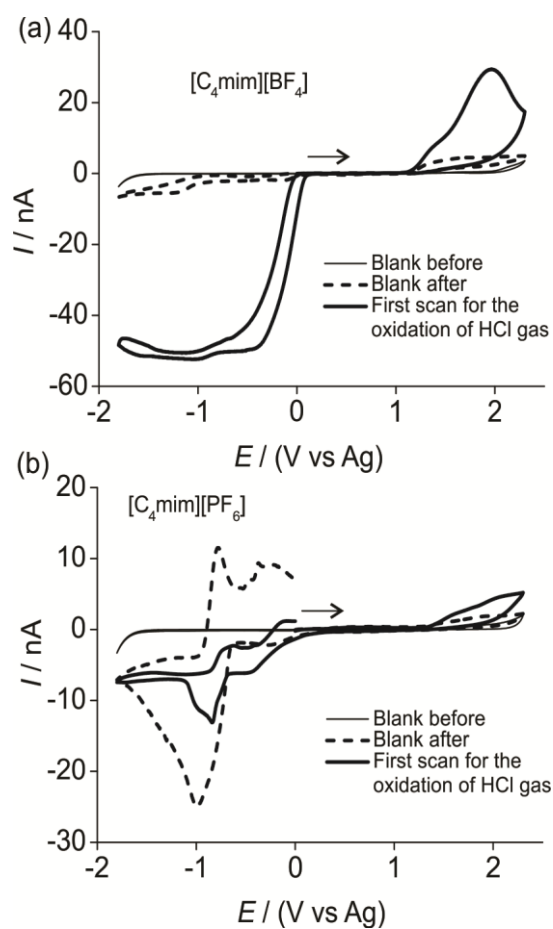


Figure 2: CVs showing changes in blank scans (RTIL under vacuum conditions) for the oxidation of 2.56 % hydrogen chloride gas on a 8.3 μm radius Pt electrode in a) $[C_4mim][BF_4]$ and b) $[C_4mim][PF_6]$ at a scan rate 0.1 V/s. The thin black line is the blank scan before HCl gas and the thick dashed line is blank scan after HCl gas experiments.

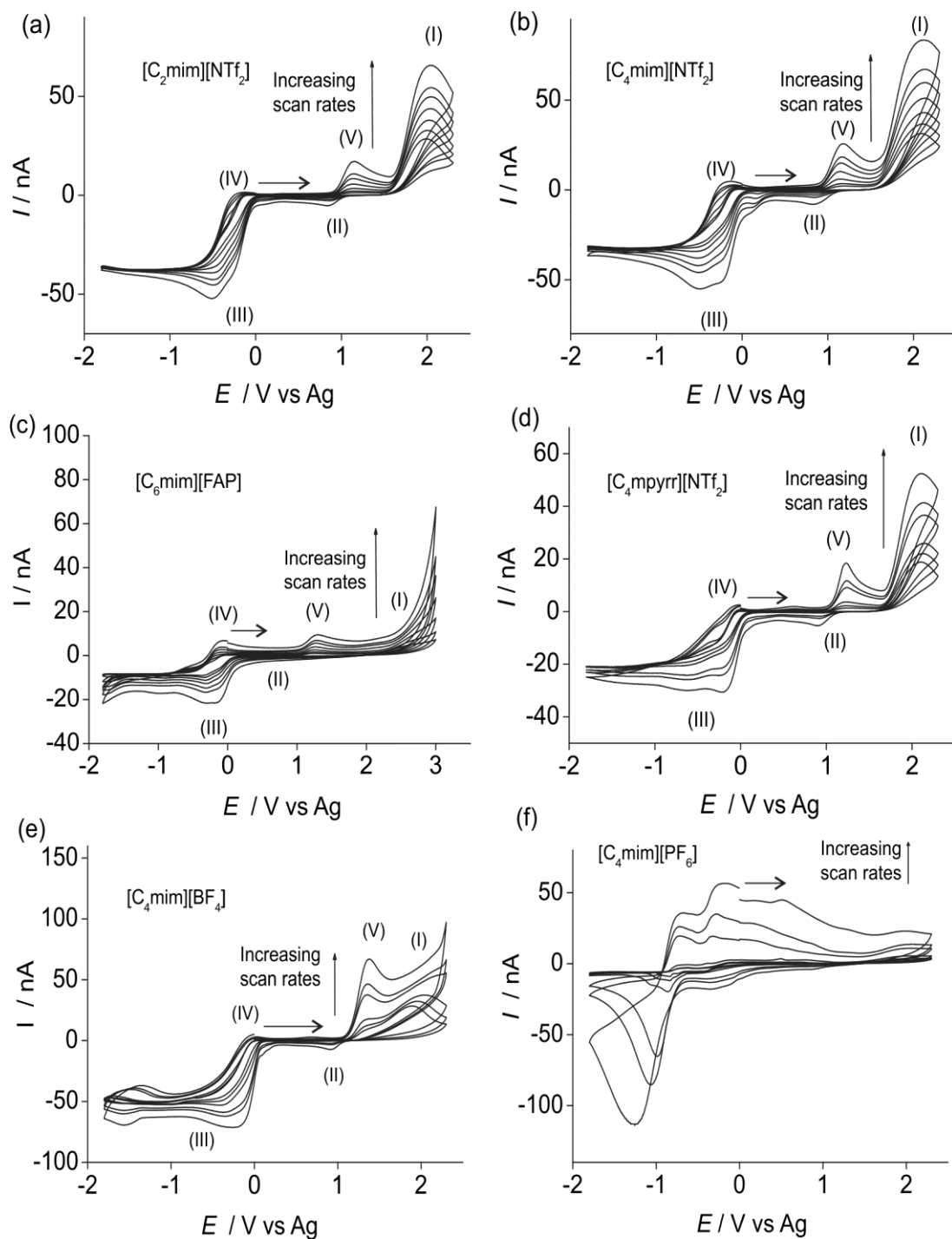


Figure 3: CVs for the oxidation (second scan) of 2.56 % hydrogen chloride gas on a 8.3 μm radius Pt electrode in a) $[\text{C}_2\text{mim}][\text{NTf}_2]$, b) $[\text{C}_4\text{mim}][\text{NTf}_2]$, c) $[\text{C}_6\text{mim}][\text{FAP}]$, d) $[\text{C}_4\text{mpyrr}][\text{NTf}_2]$, e) $[\text{C}_4\text{mim}][\text{BF}_4]$, f) $[\text{C}_4\text{mim}][\text{PF}_6]$ at various scan rates between 0.05 and 2 V/s. The labels for peaks (I) to (V) are not included for $[\text{C}_4\text{mim}][\text{PF}_6]$ (f) due to different reactions occurring in this RTIL.

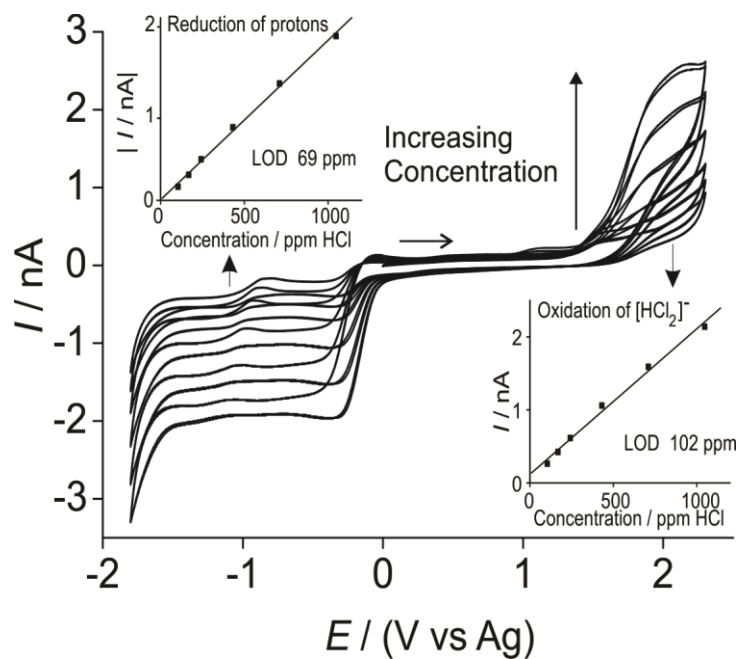


Figure 4: CVs (first and second scan) for the oxidation of different concentrations (104, 168, 242, 431, 710 and 1048 ppm) of HCl gas on a 8.3 μm radius Pt electrode in $[C_2mim][NTf_2]$ at a scan rate 0.1 V/s. Insets are calibration graphs of current for peak I (first scan) and peak III (first scan) vs. gas phase concentration.

5 References

1. R. P. Pohanish, *Sittig's Handbook of Toxic and Hazardous Chemicals and Carcinogens: A-K*, Elsevier, 2012.
2. M. J. O'Neil, *The Merck Index: An Encyclopedia of Chemicals, Drugs, and Biologicals*, Royal Society of Chemistry, 2013.
3. C. G. A. Inc., *Handbook of Compressed Gases*, Springer US, Dordrecht, The Netherlands, 1999.
4. F. J. Arnáiz, *J. Chem. Educ.*, 1995, **72**, 1139.
5. M. Michlmayr and D. T. Sawyer, *J. Electroanal Chem. Interfacial Chem.*, 1969, **23**, 387-397.
6. L. Aldous, D. S. Silvester, W. R. Pitner, R. G. Compton, M. C. Lagunas and C. Hardacre, *J. Phys. Chem. C*, 2007, **111**, 8496-8503.
7. P. Bonhôte, A.-P. Dias, N. Papageorgiou, K. Kalyanasundaram and M. Grätzel, *Inorg. Chem.*, 1996, **35**, 1168-1178.
8. D. R. MacFarlane, P. Meakin, J. Sun, N. Amini and M. Forsyth, *J. Phys. Chem. B*, 1999, **103**, 4164-4170.
9. M. Sharp, *Electrochim. Acta*, 1983, **28**, 301-308.
10. K. Murugappan, C. Kang and D. S. Silvester, *J. Phys. Chem. C*, 2014, **118**, 19232-19237.
11. K. Murugappan, D. W. M. Arrigan and D. S. Silvester, *J. Phys. Chem. C*, 2015, **119**, 23572-23579.
12. L. E. Barrosse-Antle, A. M. Bond, R. G. Compton, A. M. O'Mahony, E. I. Rogers and D. S. Silvester, *Chem. Asian J.*, 2010, **5**, 202-230.
13. K. Murugappan and D. S. Silvester, *Sensors*, 2015, **15**, 26866-26876.
14. R. P. Swatloski, J. D. Holbrey and R. D. Rogers, *Green Chem.*, 2003, **5**, 361-363.
15. D. S. Silvester, L. Aldous, C. Hardacre and R. G. Compton, *J. Phys. Chem. B*, 2007, **111**, 5000-5007.
16. I. G. Shenderovich, S. N. Smirnov, G. S. Denisov, V. A. Gindin, N. S. Golubev, A. Dunger, R. Reibke, S. Kirpekar, O. L. Malkina and H.-H. Limbach, *Ber. Bunsenges. Phys. Chem.*, 1998, **102**, 422-428.
17. M. C. Buzzeo, R. G. Evans and R. G. Compton, *ChemPhysChem*, 2004, **5**, 1106-1120.